Investigation on the Structure and Optical Properties of Fe^{2+}:ZnSe Quantum Dots Synthesized by Microemulsion Method

Leilei Ma[1], Ying Sun[2, *]

[1]College of Chemical Engineering, Shenyang University of Chemical Technology. Shenyang, 110142, China.

[2]The Faculty of Social Sciences and Humanities, National University of Malaysia. Bangi Selangor, 43600, Malaysia.

*Corresponding: P153029@siswa.ukm.edu.my

Accepted: 10-12-2024 Published: 10-01-2025

Abstract

ZnSe quantum dots (QDs) have intensively studied because of their unique optical properties and enormous applications. By doping transition metal ions in ZnSe QDs, their properties can be further optimized and new functions can be given. In this work, Fe^{2+} doped ZnSe QDs were successfully prepared using inverse microemulsion-assisted hydrothermal method, and advanced characterization methods were used to systematically study their structure and optical properties. The research results showed that Fe^{2+} was successfully doped into the ZnSe lattice, and with the increase of Fe^{2+} doping concentration, the particle size of QDs gradually decreased. The actual doping ratio of Fe^{2+} was about 41% of the initial concentration. Optical properties studies showed that Fe^{2+} doping reduced the band gap width of ZnSe QDs from 2.43 eV to 1.96 eV. The synthesis of Fe^{2+} doped ZnSe QDs provides new possibilities for its application in optoelectronic devices and photocatalysis.

Keywords: ZnSe; Fe^{2+}:ZnSe; Quantum dots; Optical properties

Highlights

• Fe^{2+} doped ZnSe quantum dots were successfully prepared using inverse microemulsion-assisted hydrothermal method.

• The structure and optical properties of the QDs were investigated in details.

• The relationship between the true doping concentration of Fe^{2+} and the luminescence performance was deeply studied.

Introduction

In recent years, semiconductor quantum dots (QDs) have garnered significant attention due to their unique optical and electronic properties, which arise from quantum confinement effects[1, 2]. Among these, zinc selenide (ZnSe) QDs have emerged as a promising material due to their wide bandgap, high photoluminescence efficiency, and excellent stability[3]. These characteristics make ZnSe QDs highly suitable for a variety of applications, including optoelectronic devices[4], biomedical imaging[5], and photocatalytic systems[6, 7]. The exploration of ZnSe QDs has led to remarkable advancements in synthesis techniques, surface modification, and doping strategies. Improved methods such as hot-injection and hydrothermal synthesis have enabled the production of QDs with superior monodispersity and precise size control[8, 9]. Additionally, surface passivation and functionalization have enhanced their stability and fluorescence efficiency, broadening their applicability[10]. Doping with transition metals or rare-earth elements has further optimized their optoelectronic properties, making them more effective in practical applications[11-13].

By introducing transition metal ion doping, the properties and applications of ZnSe quantum dot materials can be effectively improved. Mn^{2+} doping of ZnSe QDs can enhance fluorescence quantum efficiency and orange light emission applications[14]; The stability of QDs doped with Cu^{2+} is significantly improved in light, heat, and chemical environments[10]. Transition metal ion doped quantum dots not only exhibit excellent optical properties, but also exhibit magnetic, catalytic, and other characteristics[15, 16].

Although significant progress has been made in the doping of ZnSe QDs with transition metal ions, there are still challenges such as difficulty in accurately controlling the distribution and concentration of doping ions, which affects the performance of QDs; The synthesis process of high-quality doped QDs is complex, costly, and difficult to produce on a large scale; Further research is needed to improve the luminescence efficiency, catalytic activity, and magnetism of doped QDs.

Based on this, this paper developed a reverse micellar microemulsion assisted hydrothermal method to generate Fe^{2+} doped ZnSe QDs. Through advanced material physical and chemical performance analysis and spectral characterization, we understand the relationship between the true doping concentration of Fe^{2+} and the luminescence performance, and then improve the performance of Fe^{2+} doped ZnSe QDs materials.

Experimental

Sodium borohydride ($NaBH_4$, ≥98.5%), selenium powder (Se, 99.999%), $Zn(CH_3COO)_2$ (99.9%), $FeSO_4·7H_2O$, Triton X-100, cyclohexane (anhydrous, 99.5%), 2-propanol (99.5%) were used as raw materials. The preparation of nano-sized powder was carried out using a microemulsion-mediated hydrothermal method. The microemulsion medium was prepared by mixing Triton X-100, 2-propanol, and cyclohexane in a volume ratio of 3:5:20.

Under an inert gas atmosphere, 5.0 mmol of $Zn(CH_3COO)_2$ and varying molar amounts of $FeSO_4·7H_2O$ were dissolved in 8 ml of deionized water. The microemulsion was then injected to form the cationic precursor solution, designated as M_A. Separately, a quantity of 10.4 mmol of $NaBH_4$ was dissolved in 10 ml of deionized water and stirred until a clear solution was obtained. Selenium powder, equivalent to the total cationic molar amount, was added to the $NaBH_4$ solution. Upon completion of the reaction, a light white cloud formed, indicating the formation of NaHSe. The microemulsion medium was then added to this solution to form anionic precursor solution, designated as M_B.

The two precursor solutions (M_A and M_B) were mixed and stirred for half an hour at room temperature under an inert gas atmosphere. The mixture was subsequently transferred to a 100 mL Teflon-lined high-pressure reactor and subjected to hydrothermal treatment at 120°C for 12 hours without stirring to ensure sufficient crystallization of the quantum dots. After the reaction, the system was allowed to cool naturally to room temperature.

In the microemulsion system (M_A), the concentration of $Zn(CH_3COO)_2$ was kept constant, while the molar ratio of $FeSO_4·7H_2O$ to $Zn(CH_3COO)_2$ was adjusted to 0.02, 0.05, 0.08, and 0.1. The resulting precipitate was separated from the reaction medium by centrifugation, washed multiple times with deionized water and anhydrous ethanol, and then vacuum-dried. This procedure enabled the preparation of ZnSe samples with varying levels of Fe^{2+} doping, designated as 0.02Fe:ZnSe, 0.05Fe:ZnSe, 0.08Fe:ZnSe and 0.1Fe:ZnSe.

X-ray diffraction (XRD) pattern of the samples were obtained by an Empyrean-100 Panalytical diffractometer using monochromatic Cu Kα irradiation (1.5418 Å). X-ray photoelectron spectroscopy (XPS) studies were carried out on Thermo Scientific K-Alpha using an Al Kα monochromated source. To achieve high precision measurements of elements concentration, Inductively Coupled Plasma Optical Emission Spectrometer (ICP-OES) measurements were carried out using a PerkinElmer Avio 550 Max system. Ultraviolet Visible (UV-Vis) absorption spectra were measured using a Lambda 950 spectrometer in the range from 200 to 800 nm with a measurement step of 1 nm. The steady-state excitation and emission spectra were obtained using a FLS 1000 fluorescence spectrometer (Edinburgh) with a xenon lamp serving as the excitation source. Background subtraction, excitation correction, and emission correction were meticulously verified using the software.

Results and Discussion

Fig. 1 displays the XRD pattern of ZnSe and Fe:ZnSe QDs. It is evident that samples exhibit a sphalerite structure, with three main peaks observed at 27.2°, 45.2°, and 53.6°, corresponding to the (111), (220), and (311) planes of the cubic sphalerite crystal structure[17], which aligns well with the standard card (JCPDS no. 65-9602). The substitution of Zn^{2+} ions ($r_{Zn}{}^{2+}$ = 0.74 Å) with the smaller radius Fe^{2+} ions ($r_{Fe}{}^{2+}$ = 0.72 Å) doesn't impact the lattice structure of ZnSe substrate. With the increase in Fe^{2+} doping content, the intensity of the (111) crystal plane decreases and its position shifts towards higher diffraction angles. This phenomenon indicates that Fe^{2+} is incorporated into the lattice of ZnSe. The crystallite size of the samples was analyzed using the Debye-Scherrer equation, with the results presented in Fig. 2, which is smaller than the Bohr exciton diameter (9.0 nm) of bulk ZnSe[18], indicating that these QDs in this study are in a strong quantum confinement regime. This indicates that ZnSe QDs doped with different concentrations of Fe^{2+} has been successfully synthesized.

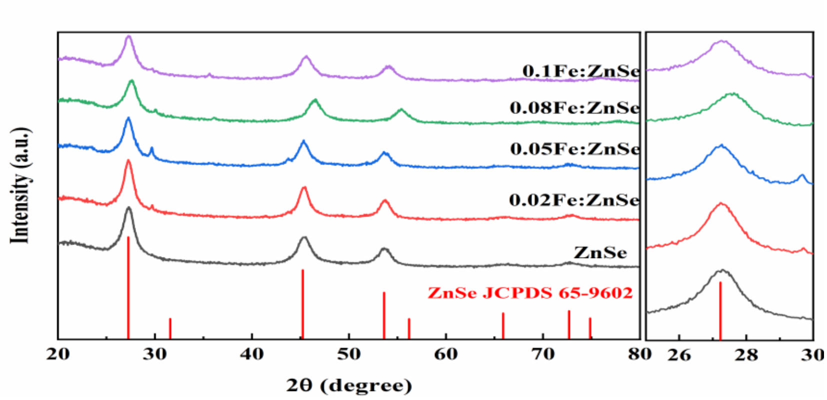

Fig. 1. XRD patterns of synthesized ZnSe and Fe:ZnSe QDs, the right image is an enlarged view of the ZnSe (111) crystal plane.

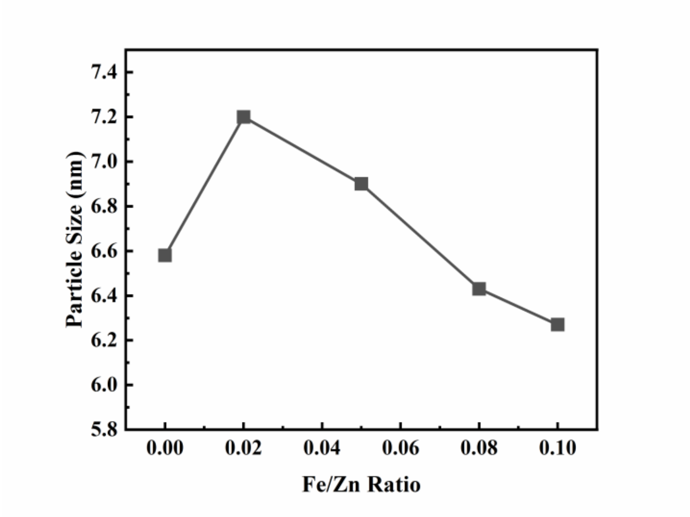

Fig. 2. The particle size of ZnSe and Fe:ZnSe samples.

The XPS analysis investigated the surface composition and chemical states of ZnSe and Fe:ZnSe QDs, as shown in Fig. 3. The XPS spectrum for Zn 2p exhibited two main peaks with binding energies of 1021.6 eV and 1044.6 eV, corresponding to Zn $2p_{3/2}$ and Zn $2p_{1/2}$, respectively[19, 20]. A fine scan of Se revealed a composite peak, displaying splitting of the $3d_{5/2}$ and $3d_{3/2}$ levels with binding energies of 53.4 eV and 54.1 eV, indicating that Se exists as a -2 valence ion. It is noteworthy that the characteristic peaks for Fe are not as strong as those of other elements, which can be attributed to the low doping amount of Fe and its incorporation within the QDs matrix. The Fe 2p orbital exhibits typical spin-orbit splitting characteristics. The binding energies at 709 eV and 724.6 eV correspond to Fe $2p_{3/2}$ and Fe $2p_{1/2}$, respectively[21-23], confirming the successful doping of Fe into the ZnSe nanocrystals. There exists two satellite peaks at 714.5 eV and 721.5 eV. Which are used to distinguish the charge states of Fe atoms in compound materials. Satellite peak 1, with a binding energy of 714.5 eV, offers clear evidence for the existence of Fe^{2+}. Satellite peak 2, with a binding energy of 721.5 eV, can be assigned to the characteristic peaks of Fe^{3+}; its peak intensity is very weak, compared with satellite peak 1, which indicates that the amount of Fe^{3+} is extremely small in the iron-doped ZnSe matrix.

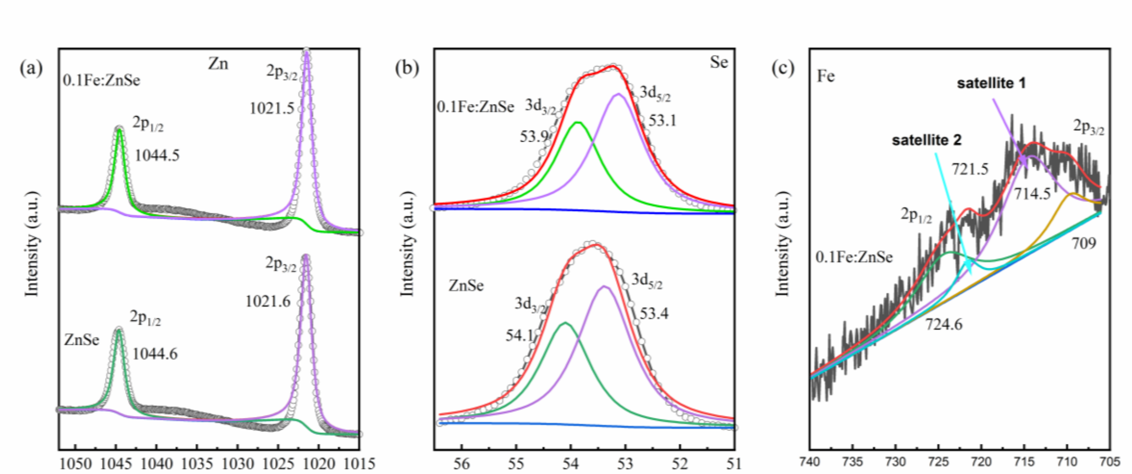

Fig. 3. High resolution XPS spectra of Zn 2p (a) and Se 3d (b) for ZnSe and 0.1Fe:ZnSe samples (The circle-lines are experimental data, and the colored lines are fitting data). (c) High resolution XPS spectra of Fe 2p for 0.1Fe:ZnSe sample (The black line is experimental data while colored lines are fitting data)

To further determine the actual concentration of Fe^{2+} in QDs with different initial Fe/Zn doping ratios, ICP-OES was employed to measure the atomic concentration percentage of Fe in the Fe:ZnSe QDs, as shown in Fig. 4. Previous studies[24]have shown that during the hydrothermal synthesis of Fe^{2+} doped ZnSe nanoparticles, hydrothermal treatment time and temperature can significantly affect the actual doping concentration of Fe^{2+}. In this study, the temperature and time for different concentrations of Fe^{2+} doped ZnSe were kept constant. Therefore, the primary factor affecting the actual Fe^{2+} doping ratio was the initial concentration of Fe^{2+}. From Fig. 4, it can be observed that as the initial Fe^{2+} doping concentration increases, the actual atomic ratio of Fe gradually declines from 44% to 41%. On the one hand, the result indicates that Fe^{2+} has successfully doped into the

ZnSe QDs; on the other hand, with the increase of Fe^{2+} concentration, it takes a longer time or higher temperature assisted Fe^{2+} to enter the ZnSe lattice. Since the temperature and time remained unchanged in this study, the high concentration of Fe^{2+} may not have been fully accommodated. Nevertheless, the overall doping ratio remains above 41%, which is relatively high compared to similar syntheses reported in the literature[24], indicating a substantial level of doping achieved in this work.

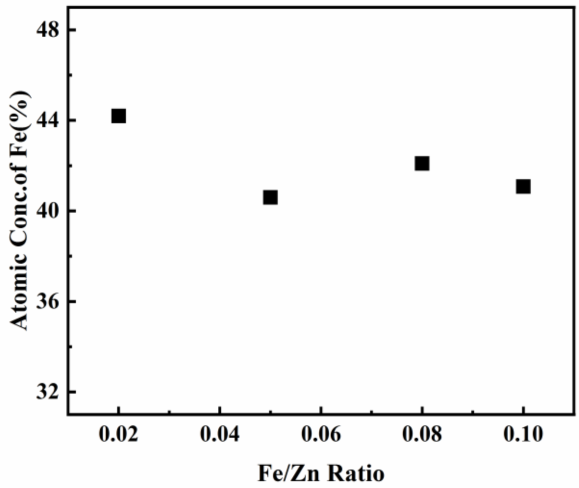

Fig. 4. Actual and theoretical ratios of Fe atom in Fe:ZnSe samples with different Fe/Zn ratios.

The UV-Vis absorption spectra of pure ZnSe and Fe:ZnSe QDs are presented in Fig. 5(a). The spectrum of pure ZnSe exhibits an absorption peak at 460 nm, which corresponds to the characteristic band-edge absorption of ZnSe[25], with a bandgap value of 2.43 eV. Upon doping with Fe^{2+}, the band edge absorption of ZnSe initially undergoes a blue shift. This phenomenon is attributed to the quantum size effect altering the dimensions of the ZnSe nanocrystals[21, 25]. The absorption band from 500 nm to 700 nm belongs to the excitonic absorption of Fe^{2+} ions ($Fe^{2+} + h\nu \rightarrow Fe^{1+} + h_{VB}$), confirming the existence of Fe^{2+} ions in the Fe:ZnSe QDs[17]. The bandgap values of Fe:ZnSe samples with varying doping concentrations were calculated using the Tauc equation, as shown in Fig. 5(b). It can be observed that with increasing concentrations of Fe^{2+}, the bandgap gradually decreases. When the doped molar amount of Fe element is 0.1, the bandgap is reduced to 1.96 eV.

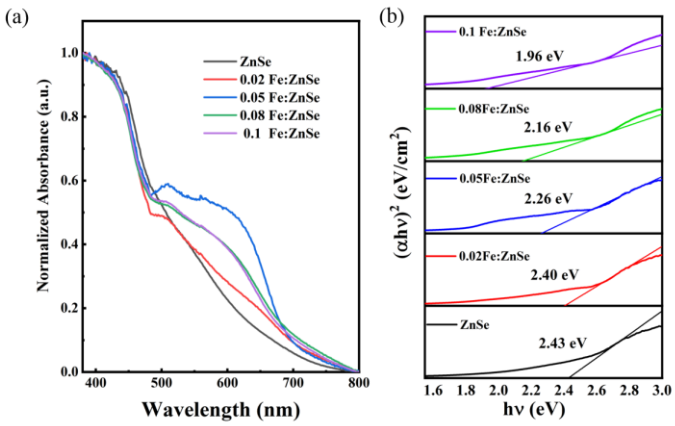

Fig. 5. Normalized absorption spectra (a) and Tauc plots curves (b) of ZnSe and Fe:ZnSe samples, bandgap energies are plotted on the figure, respectively.

To characterize the differences in optical properties between ZnSe and Fe^{2+}:ZnSe QDs, steady-state fluorescence spectroscopy was performed. The emission spectra for ZnSe and Fe^{2+}:ZnSe samples were obtained using an excitation wavelength of 340 nm, and the results are shown in Fig. 6(a). All samples exhibit emission peaks in the visible light region: a blue light emission peak located about 440 nm, attributed to near-band edge luminescence of ZnSe[21, 26-28].

Upon the introduction of iron ions, the Fe:ZnSe samples with varying doping concentrations exhibit one fluorescent emission peaks attributed to the band edge luminescence of ZnSe. The emission peak center at about 440 nm shows a phenomenon of redshift first and then blueshift., which is due to the variation in the size of the ZnSe nanocrystals, resulting in a stronger quantum confinement effect, an increase in particle size leads to a red shift, while a decrease in particle size results in a blue shift[29].

Fig. 6(b) presents the excitation spectra of the relevant samples at an emission wavelength center about 440 nm, which shows two excitation peaks at 250 nm, and 375 nm, With the Fe^{2+} doping concentration increasing, the intensity of the emission peak center at 250 nm gradually weakens. However, when the doping concentration is 0.1, the intensity surges to the maximum. The intensity of the 250 nm emission peak shows a non-monotonic variation with doping. The broadband excitation peak at 375 nm exhibits a red shift and changes in intensity, the Fe^{2+} doped samples display a predominant excitation peak centered around 375 nm (excluding the 0.05 Fe:ZnSe sample). This observation further indicates that the ZnSe and Fe:ZnSe prepared have potential applications in light-emitting devices, photocatalysis and other fields.

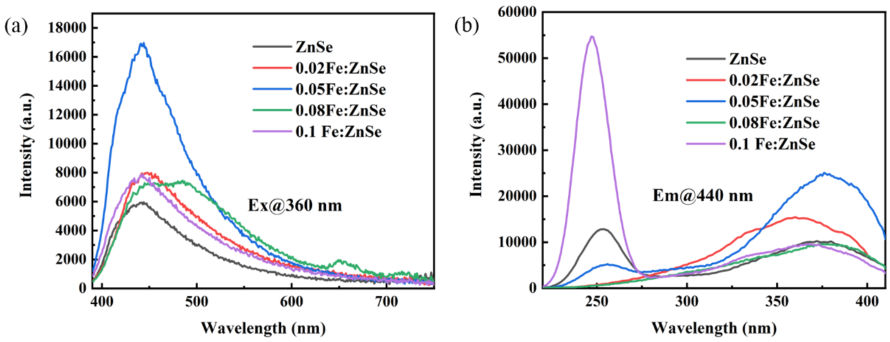

Fig. 6. (a) Emission spectra of ZnSe and Fe:ZnSe series samples under 360 nm excitation; Excitation spectra of ZnSe and Fe:ZnSe samples monitored at 440 nm (b)

Conclusion

In this work, Fe^{2+} doped ZnSe QDs were successfully prepared using inverse microemulsion-assisted hydrothermal method. The introduction of iron ions leads to the reduction of the size of ZnSe, and the sizes of these QDs are in the nanometer level, showing strong quantum confinement characteristics. The true proportion of Fe^{2+} doping into ZnSe lattice is more than 41%. The introduction of Fe^{2+} reduces the bandgap of ZnSe semiconductor from 2.43 eV to 1.96 eV, These Fe^{2+} doped ZnSe QDs materials have potential applications in light-emitting devices, photocatalysis and other fields.

Conflicts of interest

The authors declare that they have no known competing financial interests or personal relationships that could have appeared to influence the work reported in this paper.

CRediT authorship contribution statement

Leilei Ma: Conceptualization, Investigation, Methodology, Data curation, Formal analysis, Writing – original draft, Writing – review & editing. Ying Sun: Project administration.

Declaration of competing interest

The authors declare that they have no known competing financial interests or personal relationships that could have appeared to influence the work reported in this paper.

Acknowledgments

This research did not receive any specific grant from funding agencies in the public, commercial, or not-for-profit sectors.

References

[1] Liu G, Zhang S, Xu L, et al. Recent advances of eco-friendly quantum dots light-emitting diodes for display [J]. Progress in Quantum Electronics, 2022, 86: 100415.
[2] Jin L, Selopal G S, Sun X W, et al. Core-Shell Colloidal Quantum Dots for Energy Conversion [J]. Advanced Energy Materials, 2024, 15(1): 2403574.

[3] Deng X, Zhang F, Zhang Y, et al. Heavy-metal-free blue-emitting ZnSe(Te) quantum dots: synthesis and light-emitting applications [J]. Journal of Materials Chemistry C, 2023, 11(42): 14495-14514.
[4] Gu L, Li X, Xia L, et al. Colloidal Quantum Dots-Based Photoelectrochemical-Type Optoelectronic Synapse [J]. Advanced Functional Materials, 2024, 35(6): 2415178.
[5] Jebakumar D S I, Jenison D S. Zinc selenide quantum dots as fluorescent labels for iomedical imaging [J]. Applied Organometallic Chemistry, 2024, 38(3): e7357.
[6] Xin Z, Huang M, Wang Y, et al. Reductive Carbon–Carbon Coupling on Metal Sites Regulates Photocatalytic CO_2 Reduction in Water Using ZnSe Quantum Dots [J]. 2022, 61(31): e202207222.
[7] Kuehnel M F, Sahm C D, Neri G, et al. ZnSe quantum dots modified with a Ni(cyclam) catalyst for efficient visible-light driven CO_2 reduction in water [J]. Chemical Science, 2018, 9(9): 2501-2509.
[8] Nguyen D H, Kim S H, Lee J S, et al. Reaction-dependent optical behavior and theoretical perspectives of colloidal ZnSe quantum dots [J]. Scientific Reports, 2024, 14(1): 13982.
[9] Malik K, Assadullah I, Malik J, et al. Growth and properties of hydrothermally derived crystalline ZnSe quantum dots [J]. Environmental Science and Pollution Research, 2021, 28(4): 3953-3959.
[10] Zhang J, Zhang Z, Zhang S, et al. Efficient photoluminescence from Cu^{2+} doped ZnSe/ZnS core-shell quantum dots in silicate glass [J]. Journal of Non-Crystalline Solids, 2023, 606: 122225.
[11] Song X, Qin Y, Yu C, et al. Construct ZnSeTe/ZnTe Nanostructures with the Tunable Emission from 450 to 760 nm [J]. Journal of Physical Chemistry Letters, 2025, 16(4): 1045-1050.
[12] Hassan H H. The optical and luminescence properties of Hf-doped ZnSe QDs with multiple emission colors for light emitting devices applications [J]. Optik, 2021, 242: 167346.
[13] Bluwi A, Sarah A, Shirbeeny W. The luminescence characteristics of multicolors-tunable $Zn_{1-x}Er_xSe$ QDs prepared via microwave irradiation technique for light emitting diode applications [J]. Optik, 2020, 223: 165644.
[14] Zhang Z, Zhang T, Wang J, et al. Photoluminescence from Cu / Mn: ZnSe quantum dots and their phase transformation in silicate glass [J]. Journal of Luminescence, 2023, 258: 119766.
[15] Zhang Y, Shen Y, Wang X, et al. Enhancement of blue fluorescence on the ZnSe quantum dots doped with transition metal ions [J]. Materials Letters, 2012, 78: 35-38.
[16] Saha A, Makkar M, Shetty A, et al. Diffusion doping in quantum dots: bond strength and diffusivity [J]. Nanoscale, 2017, 9(8): 2806-2813.
[17] Shi H, Xiao X, Xu S, et al. Cobalt and iron co-doped ZnSe nanocrystals:Mid-IR luminescence at room temperature [J]. Autonomic neuroscience: basic & clinical, 2020, 221(1): 117102.
[18] Xie R, Zhang X, Liu H. Ligand-assisted fabrication, structure, and luminescence properties of Fe:ZnSe quantum dots [J]. Materials Science and Engineering: B, 2014, 182: 86-91.
[19] Cortaza M A, Morales E R, Castillo S, et al. Microwave-assisted hydrothermal synthesis of type II ZnSe/ZnO heterostructures as photocatalysts for wastewater treatment [J]. Ceramics International, 2023, 49(14): 24027-24037.
[20] Yang L, Zhu J, Xiao D. Synthesis and characterization of ZnSe:Fe/ZnSe core/shell nanocrystals [J]. Journal of Luminescence, 2014, 148: 129-133.
[21] Li T, Sun C, Xue C, et al. Structure and optical properties of iron doped ZnSe microspheres [J]. Optical Materials, 2021, 114: 110989.
[22] Nan W, Yang D, Zhou B, et al. Luminescence Properties of Fe^{2+}:ZnSe Single Crystals Grown via a Traveling Heater Method [J]. Crystals, 2023, 13(3): 411.
[23] Yamashita T, Hayes P. Analysis of XPS spectra of Fe^{2+} and Fe^{3+} ions in oxide materials [J]. Applied Surface Science, 2008, 254(8): 2441-2449.
[24] Wang J, Boeckl J, Wheeler R, et al. Synthesis and size control via variation of temperature of ZnSe:Fe nanocrystals in a microemulsion assisted hydrothermal system [J]. Materials Chemistry and Physics, 2022, 276: 125188.
[25] Xie R, Li L, Li Y, et al. Fe:ZnSe semiconductor nanocrystals: Synthesis, surface capping, and optical properties [J]. Journal of Alloys and Compounds, 2011, 509(7): 3314-3318.
[26] Yang L, Zhu J, Xiao D. Microemulsion-mediated hydrothermal synthesis of ZnSe and Fe-doped ZnSe quantum dots with different luminescence characteristics [J]. RSC Advances, 2012, 2(21): 8179-8188.
[27] Mosmer F, Torkamany M J, Sabbaghzadeh J, et al. Optical Properties of Pure ZnSe Nanocrystals Synthesized by Laser Ablation in Organic Liquids [J]. Journal of Cluster Science, 2013, 24(3): 905-914.
[28] Feng B, Cao J, Han D, et al. ZnSe nanoparticles of different sizes: Optical and photocatalytic properties [J]. Materials Science in Semiconductor Processing, 2014, 27: 865-872.
[29] Huang S. The study of optical characteristic of ZnSe nanocrystal [J]. Applied Physics B, 2006, 84(1-2): 323-326.